Dynamical system approach to phyllotaxis

D'ovidio, Francesco; Mosekilde, Erik

Published in:
Physical Review E. Statistical, Nonlinear, and Soft Matter Physics

Link to article, DOI:
10.1103/PhysRevE.61.354

Publication date:
2000

Document Version
Publisher's PDF, also known as Version of record

Dynamical system approach to phyllotaxis

F. d'Ovidio[1,2,*] and E. Mosekilde[1,†]
[1]*Center for Chaos and Turbulence Studies, Building 309, Department of Physics, Technical University of Denmark, 2800 Lyngby, Denmark*
[2]*International Computer Science Institute, 1947 Center Street, Berkeley, California 94704-1198*
(Received 13 August 1999)

This paper presents a bifurcation study of a model widely used to discuss phyllotactic patterns, i.e., leaf arrangements. Although stable patterns can be easily obtained by numerical simulations, a stability or bifurcation analysis is hindered by the fact that the model is defined by an algorithm and not a dynamical system, mainly because new active elements are added at each step, and thus the dimension of the ''natural'' phase space is not conserved. Here a construction is presented by which a well defined dynamical system can be obtained, and a bifurcation analysis can be carried out. Stable and unstable patterns are found by an analytical relation, in which the roles of different growth mechanisms determining the shape is clarified. Then bifurcations are studied, especially anomalous scenarios due to discontinuities embedded in the original model. Finally, an explicit formula for evaluation of the Jacobian, and thus the eigenvalues, is given. It is likely that problems of the above type often arise in biology, and especially in morphogenesis, where growing systems are modeled.

PACS number(s): 05.45.−a, 87.18.La

I. INTRODUCTION

Phyllotaxis is the botanical term for the characteristic geometrical arrangements of leaves (and, by extension, of other botanical elements, like florets, seeds, and scales). We shall refer to all of these elements as *primordia*, as they are generically called in their early stage, or, with some abuse of the language, as *leaves*. A characteristic of phyllotaxis is the striking regularity of the spatial patterns that emerge, often related to mathematical quantities such as the Fibonacci numbers and the golden mean. This regularity has attracted significant interest among physicists and mathematicians at least since the early treatment by the Bravais brothers [1] who referred to them as *living crystals*. For a review of the history of phyllotactic theories we refer to the recent survey by Adler *et al.* [2].

Phyllotaxis can be studied from many different viewpoints, ranging from static geometrical and crystallographic considerations, over chemical reaction-diffusion equations and dynamical systems theory to experiments with genetic control or growth conditions. Here we are interested in a morphogenetical approach, in which these kinds of patterns are studied by finding a few simple rules that mimic the growth mechanisms around the apex of a plant. Primordia are modeled as points (or disks) formed at regular intervals of time (one primordium for each step) around a circle (the apex), and then moved away. Different rules can be used. However, in general this approach has some typical features.

(1) It involves a discrete time, iterative process, in which at each step a new primordium is added on the periphery of the apex, and already formed leaves are moved away;

(2) Two rules must be defined: the first one controls how already existing primordia are advected from the apex (for instance, by giving the speed); the second rule specifies how these leaves determine the angular position of the new primordium.

The first rule involves a parameter, related to Richards' plastochrone ratio [3], usually indicated with G. This is the parameter that will be varied when we come to study bifurcations in the pattern forming process.

Usually, one looks for patterns that are conserved by the dynamics, and finds some of the geometrical properties of natural patterns: angles between subsequent leaves near the golden mean (or, more generally, near noble numbers) and, connecting primordia to the neighboring ones, patterns related to Fibonacci numbers. The importance of these results is that the model shows that geometrical properties that are useful for plants for optimizing light exposure or seed packing can be explained by some general dynamical rules.

This approach was first exploited by Hofmeister in 1868 [4], and more recently by many others. Bernasconi and Boissanade [5] worked on the elements needed to obtain cylindrical phyllotactic patterns with two species, activator-inhibitor chemical systems. Green, Style, and Rennich [6] studied *de novo* initiation of patterns, inhibition, and stability from a biophysical point of view. Marzec and Kapraff derived a sufficient condition for uniform spacing of leaves connecting the model to noble numbers [7]. Douady and Couder obtained phyllotactic patterns in an experiment with magnetic droplets and a bifurcation diagram through a numerical simulation [8–11]. Koch *et al.* [12] introduced a simplified model of phyllotaxis, and described generic properties of the solutions. Levitov exploited an energetic approach on phyllotaxis [13], and showed that this kind of patterns can be obtained in flux lattices in layered superconductors [14]. Kunz [15] found analytical results about a generalization of the variational problem of Levitov and the experiment of Douady and Couder.

The present work is mainly concerned with bifurcations. Denoting the angular difference between two subsequent

*Electronic address: dovidio@ICSI.Berkeley.edu
†Electronic address: Erik.Mosekilde@fysik.dtu.dk

leaves as the *divergence angle*, a spiral phyllotactic pattern is defined as having all elements with the same divergence angle. Plotting the shared divergence angle of stable patterns versus G, one can construct a bifurcation diagram for the algorithm. Although analytical studies have been performed (especially we would like to mention the work of Levitov [13] and Koch *et al.* [12]), typical techniques from dynamical systems theory cannot be straightforwardly applied at this point, as phyllotaxis is related with a growing and expanding system. A consequence of this is that the algorithm differs from a dynamical system by the fact that it maps a vector (positions of the existing leaves) into a longer vector (positions of the existing leaves *plus* the position of the new one). Thus, for instance, new terms have been proposed, like *quasibifurcations* [13] or *asymptotic* states [12].

In the present work two main results are obtained. The first is a translation by which phyllotaxis, although associated with an expanding system, can be described in terms of ordinary dynamical system theory. Besides offering tools for the study of phyllotaxis itself, we hope that this approach can be helpful in the modeling of other analogous systems typical of morphogenesis (like embryology), where growth and expansion play a fundamental role and often seem to hinder a direct application of dynamical systems theory.

The second result is the analysis of the bifurcation phenomena that control the emergence and disappearance of patterns, and the description of the roles of different growth mechanisms (the expansion and the birth of a new element) in determining the shape. In particular, a full bifurcation diagram for stable and unstable patterns is analytically obtained, and a method for obtaining eigenvalues is given.

II. FROM THE ALGORITHM TO A DYNAMICAL SYSTEM

A. Algorithm

The algorithm studied in the present paper is based on ideas introduced by Hofmeister in 1868 and more recently revisited. In particular, we will use the set of rules proposed by Douady and Couder [10].

(1) The space is flat and two-dimensional. Elements are points, and the apex is the unit circle.

(2) The dynamics is an iterative process.

(3) At each step, already existing elements are moved away radially from the apex, increasing their radial coordinate with the relation

$$\rho \rightarrow \rho e^{G}. \tag{1}$$

(4) At each step, after moving existing elements, a new element is added on the unit circle (the apex). The angular coordinate is chosen by finding on the unit circle the absolute, leftmost minimum of an inhibitory potential generated by already existing elements. It is necessary to specify a ''right'' or ''left'' in order to resolve degenerate situations, with more than one minimum with the same value. Calling $\mathcal{M}$ the operator that gives the absolute, leftmost minimum, and using polar coordinates, the new element has

$$\rho_{new} = 1, \tag{2}$$

$$\theta_{new} = \mathcal{M}_{\alpha}(H_{\{\rho_k\},\{\theta_k\}}(\alpha)), \tag{3}$$

where where $k = 0,1,2,\ldots$ is the age of a leaf (that is, the number of steps elapsed since its formation). $H_{\{\rho_k\},\{\theta_k\}}$ is a function on the unit circle that depends on the positions of existing elements, as will be explained later.

It is important to note that, after its formation, a leaf does not change its angular position, and that the time law for the radial coordinate of the primordia is simply

$$\rho_k = e^{kG}, \tag{4}$$

To obtain Eq. (4), we have just to consider that the leaf starts with 1, and then apply Eq. (1). This relation will be important in the following, as it allows us to consider only ages and angular coordinates.

Regarding the inhibitory potential, Douady and Couder proposed using a relation in analogy with an electrostatic repulsion. Extending the sum to all the elements, and calling $d_k(\alpha)$ the distance between the kth element and a point of angular position α on the unit circle,

$$H_{\{\rho_k\},\{\theta_k\}}(\alpha) = \sum_k \frac{1}{d_{\rho_k,\theta_k}(\alpha)}. \tag{5}$$

More generally,

$$H_{\{\rho_k\},\{\theta_k\}}(\alpha) = \sum_k V(d_{\rho_k,\theta_k}(\alpha)), \tag{6}$$

where $V(d)$ can have different form, such as e^{-d}, d^{-n}, etc. It has been shown [9] that the behavior of the system is qualitatively the same for a large class of V functions. Also in this work, we will not need to define V explicitly. We will only require V to be monotonically decreasing and smooth (C^3, for simplicity, but many of our results are valid even if V is discontinuous). It is now useful to apply Eqs. (1) to (6), changing the dependence from ρ_k to kG:

$$H_{\{\rho_k\},\{\theta_k\}}(\alpha) = \sum_k V_{kG,\theta_k}(\alpha) = H_{G,\{\theta_k\}}(\alpha). \tag{7}$$

Summing up and compacting the notation, we define a parametric function that, given a set of angular coordinates, returns the angular position of the new element:

$$f_G(\{\theta_k\}) := \mathcal{M}_{\alpha}(H_{G,\{\theta_k\}}(\alpha)). \tag{8}$$

This will be the basic quantity, and we will rarely need to explicate it.

Before proceeding, we want to specify the notation and the terminology that will be used in the following. We use as synonymous the words *leaf, primordium, and element.* To indicate the angular position of the kth leaf, we use the symbol θ_k, while we will reserve the symbol θ for the whole set of coordinates (i.e., $\theta = \{\theta_k\}$). We use the term inhibitory potential for the function H_G, and we shall evaluate it on the unit circle. We use the symbol $\mathcal{M}_{\alpha}$ for the operator that gives the position of the absolute, leftmost minimum of a function of α. To indicate a general angular coordinate, we will use ϕ.

B. A straightforward modeling of the algorithm

We first rewrite the model described in Sec. II A with formal definitions, starting from leaves. At each step, leaves are in rings of radius $\rho_k = e^{Gk}$, where k represents the age of the leaf. The angular position of each leaf is determined at birth by minimizing the inhibitory potential. At each step of the dynamics, a new leaf is formed on the first ring, while all others ''jump'' from their present ring to the next, outer one. Thus we can compile all the information as a vector containing all angular positions in order of age. When we apply the dynamics, we move all the components one step ($\theta_{k+1} \rightarrow \theta_k$) and we add in the first position the angular coordinate of the new leaf. It is important to note that at each step the vector length is increased by one. For example, we start with one leaf, in $\phi = 0$:

$$\theta = (0).$$

The second leaf will grow on the opposite side of the apex:

$$\theta \rightarrow \theta = (\pi, 0).$$

The third leaf will be somewhere in between, e.g., $\pi/4$:

$$\theta \rightarrow \theta = (\pi/4, \pi, 0).$$

And so on. Thus we obtain a vector from the previous one:

$$(0) \rightarrow (\pi, 0) \rightarrow (\pi/4, \pi, 0) \rightarrow \cdots.$$

The radial coordinate is always given by $\rho_k = e^{Gk}$. This is the reason why we move a coordinate to the right: to increase ρ we have to increase the index. Also, we remark that the (angular) position of the new leaf is a function of all the already existing leaves, so, in general,

$$(\theta_0, \theta_1, \ldots, \theta_N) \rightarrow (f_G(\theta_0, \ldots, \theta_N), \theta_0, \theta_1, \ldots, \theta_N) \tag{9}$$

Here f_G is the function that finds the absolute, left-most minimum in the inhibitory potential generated by $\theta_0, \ldots, \theta_N$ as defined in Eq. (8).

Writing this as a set of equations, we can define a function that, from an N-component vector θ, generates an $(N+1)$-component vector θ':

$$\begin{aligned} \theta'_0 &= f_G(\theta), \\ \theta'_1 &= \theta_0, \\ \theta'_2 &= \theta_1, \\ &\cdots \\ \theta'_N &= \theta_{N-1}. \end{aligned} \tag{10}$$

We now introduce a modification to Eq. (10): we also apply a rotation to always have the first new leaf in the origin of the circle ($\phi = 0$):

$$\begin{aligned} \theta'_0 &= 0, \\ \theta'_1 &= \theta_0 - f_G(\theta), \\ \theta'_2 &= \theta_1 - f_G(\theta), \\ &\cdots \\ \theta'_{N+1} &= \theta_N - f_G(\theta). \end{aligned} \tag{11}$$

This will be helpful at a later stage, when we want to consider stable patterns. At this point we have something similar to a dynamical system, as we have an iterative ''map'' and a ''phase space.'' However, there is a difference: the phase space is not well defined for a dynamical system, as the vector changes its length. So Eqs. (11) are not a map from a space onto itself. To solve the problem we will proceed as follows. First we will consider the simple case in which the number leaves is upper limited, introducing a slightly different notation. Then we will extend this approach to an infinite set of leaves.

C. Representing an upper limited number of leaves

Consider a system with a maximum number of leaves (i.e. points in a bidimensional space), say $k \leqslant N$, disposed on N rings around the origin. Each ring can hold only one leaf, or none. To represent a set of leaves in this system, we can use two vectors with a component for each ring. The first will contain the angular positions of leaves, and the second will be just a place holder, each component telling, with a 0 or 1, if the corresponding ring has a leaf or nothing. So for instance, if we have only a leaf in the second ring ($i = 1$, counting from 0, and angular position ϕ) the two vectors (let us call them θ and b) will be

$$\theta = (\theta_0, \phi, \theta_2, \theta_3, \ldots, \theta_{N-1}), \quad b = (0,1,0,\ldots,0). \tag{12}$$

Note that $\theta_i, i \neq 1$ can have any value. This is clearer if, instead of two real vectors, we consider a single complex vector, b components being the radii and θ components the angular coordinates:

$$\begin{aligned} x &= x(\theta, b), \\ x_k &:= b_k e^{i\theta_k}. \end{aligned} \tag{13}$$

In this case we consider points on the unit circle or in the origin. If we do so, it is clear that angular components with $b_k = 0$ can have any value, as they all are in the origin. We also remark that the order of components in the vector is important, as the index of the coordinate tells us the radial position (the number of the circle occupied by the leaf).

D. Construction of the dynamical system

Now we apply the idea described in Sec. II C to the full model. As above, we start in the ''largest'' space that we will need; that is, a space with vectors of infinite components, more precisely, a space of successions. We will use one succession for the angular positions of leaves, and another one to track which positions are occupied by leaves and which are not. An example will clarify the idea. Let us call the first

succession θ and the second b. The succession b will be used computing f_G, for considering only those elements of θ that contain a leaf, in this way:

$$f_G(\{\theta\},\{b_k\}) = \mathcal{M}_\alpha(H_{\theta,b,G}(\alpha)) = \mathcal{M}_\alpha\left(\sum_{k=0}^{\infty} V_{kG,\theta_k}(\alpha) b_k\right). \tag{14}$$

We start as usual with one leaf in zero. This means $\theta_0 = 0$. To show that we have only the first leaf, the succession b will be

$$b = \{b_0 = 1, b_k = 0 \quad k > 0\}.$$

Meanwhile, the elements of θ other than the first can be of any value: in fact, when we evaluate f_G, we will consider only elements for which b is equal to 1: the others, being multiplied by $b_k = 0$ are deleted. In other terms, if we use the complex notation as in Eq. (13), the angular positions of elements with vanishing b component are unimportant as they are all mapped into the origin. For the second step,

$$\theta_0 = 0, \quad \theta_1 = -\pi, \quad b = \{b_0 = 1, b_1 = 1, b_k = 0 \quad k > 1\}$$

and so on. We can conclude as follows.

Proposition 1. Consider the set X of pairs,

$$x \in X \Leftrightarrow x = \{\theta, b\}, \tag{15}$$

where

$$\theta = \{\theta_k\}_{k=0}^{\infty}, \quad b = \{b_k\}_{k=0}^{\infty}, \quad \theta_k \in [0, 2\pi), \quad b_k \in \{0,1\}. \tag{16}$$

Consider the map T acting on X, defined as follows:

$$x \to Tx, \tag{17}$$

$$\begin{aligned} &\theta_0 \to 0, \\ &\theta_n \to \theta_{n-1} - f_G(\theta, b), \quad n > 0, \\ &b_0 \to 1, \\ &b_n \to b_{n-1}, \quad n > 0. \end{aligned} \tag{18}$$

Then Eqs. (15)–(17) define a (discrete time, infinite-dimensional) dynamical system.

We make the following remarks.

(1) By now, we have only written the phyllotactic algorithm in a different form, such that it explicitly appears as a dynamical system. As we have not required any properties from the f_G function (the function that gives the coordinate of the new leaf), this construction can be applied to a large class of phyllotactic models.

(2) The two rules of the algorithm, the growth and the inhibitory interaction, are decoupled, one determining a shift and the other the value of the new element. This separation will be a persistent characteristic of the model. In particular, in Sec. III we show how this fact is reflected in the determination of fixed points.

III. STABLE PATTERNS AND FIXED POINTS

The above construction is useful in the sense that it places the phyllotactic model in a ''standard'' theoretical frame, thus allowing us to apply typical techniques. Here we want to find all the stable and unstable patterns. To obtain this we simply look for fixed points. The condition is

$$Tx = x. \tag{19}$$

Applying this condition to Eq. (17), we obtain

$$\begin{aligned} &\theta_0 = 0, \\ &\theta_n = \theta_{n-1} - f_G(\theta, b), \quad n > 0, \\ &b_0 = 1, \\ &b_n = b_{n-1}, \quad n > 0. \end{aligned} \tag{20}$$

This, by induction, means

$$\begin{aligned} &\theta_0 = 0, \\ &\theta_1 = \theta_0 - f_G(\theta, b) = -f_G(\theta, b), \\ &\theta_2 = \theta_1 - f_G(\theta, b) = -2 f_G(\theta, b), \\ &\ldots \\ &\theta_n = \theta_{n-1} - f_G(\theta, b) = -n f_G(\theta, b), \\ &\ldots \\ &b_0 = 1, \\ &b_1 = b_0 = 1, \\ &b_2 = b_1 = 1, \\ &\ldots \\ &b_n = b_{n-1} = 1, \\ &\ldots. \end{aligned} \tag{21}$$

Hence we have obtained the following result.

Proposition 2. A point (pattern) $x = \{\theta, b\}$ is a fixed point of T if

$$\begin{aligned} &\theta_n = -n\phi, \quad n \geqslant 0, \\ &b_n = 1, \quad n \geqslant 0, \end{aligned} \tag{22}$$

with

$$\phi = f_G(\theta, b). \tag{23}$$

We make the following remarks.

(1) The second condition of Eq. (22) tells just that all leaves must be formed (in this sense, as should be expected, proposition 2 gives the ''limit'' pattern, with infinite elements).

(2) From Eqs. (22) and (23) we can clearly see that the growth and the inhibitory interaction play two different and *independent* roles. The growth limits the class of fixed points to the set of patterns described by Eq. (22); the interaction, by Eq. (23), chooses the global parameter for the particular pattern among this class. In other words, and from a biologi-

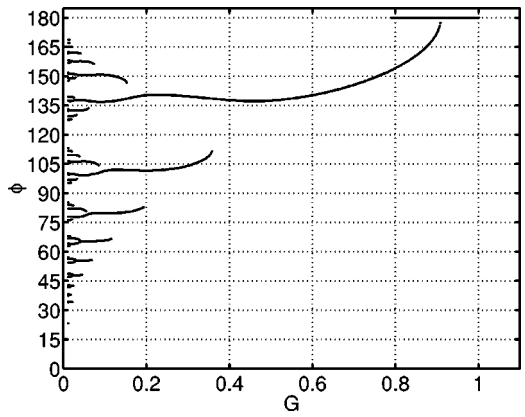

FIG. 1. Bifurcation diagram for fixed points (stable and unstable). The picture is obtained by solving the equation $F_G(\phi) - \phi = 0$ numerically. The value of ϕ is expressed in degrees.

cal point of view, a different interaction will change the divergence angles of the fixed patterns, but not the spiral shape.

(3) We can easily see that a stable pattern can only be a spiral [in fact, it must be a fixed point and thus have the form $\theta_n = -n\phi$; if we calculate the divergence angle for any leaf, we obtain the same value $f_G(\theta, b)$].

(4) It is important to recall that here we have considered fixed points only, and not cycles or more complex structures. So, in principle, other nonequilibrium stable shapes, different from spirals, can arise. This actually has been observed. See, for instance, Ref. [16] for cycles coming from a period-doubling bifurcation.

(5) The first condition gives a necessary and sufficient condition for the divergence angle of a spiral to be a fixed point.

The importance of the last remark becomes clear if we take a couple of steps more. First, we consider f_G restricted to spirals, that is, to points in which each leaf has the same divergence angle and in which all leaves are formed:

$$F_G(\phi) := f_G(\theta, b), \tag{24}$$

$$\theta_n = -n\phi, \quad b_n = 1, \quad n \geq 0. \tag{25}$$

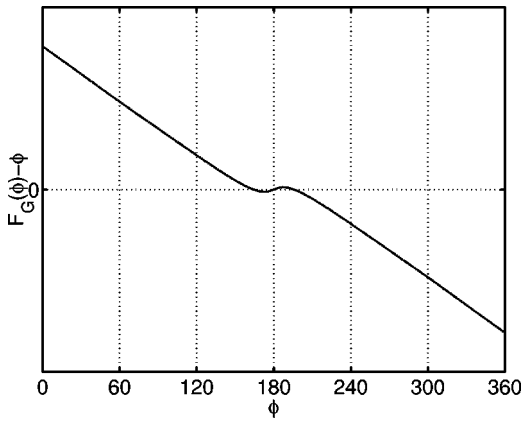

FIG. 2. Plot of the function $F_G(\phi) - \phi$ for $G = 0.87$ (values of ϕ in degrees). Two symmetric solutions appear as the function begins to fold.

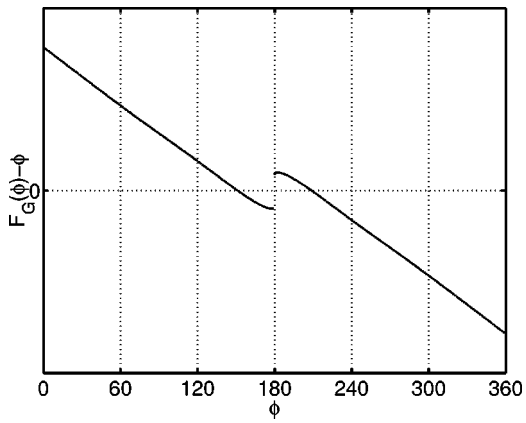

FIG. 3. Plot of the function $F_G(\phi) - \phi$ for $G = 0.77$ (values of ϕ in degrees). As the parameter G is reduced, the fold becomes sharper, and finally breaks into a discontinuity, as in the inhibitory potential a minimum is changed into a maximum (see Fig. 4).

Then the condition

$$\phi = f_G(\theta, b)$$

becomes

$$F_G(\phi) = \phi. \tag{26}$$

This is an equation in just one variable and one parameter. The solutions to this equation gives the divergence angles of all the fixed points, that is, of all the stable and unstable patterns. Plotting $F_G(\phi) - \phi = 0$ in the (G, ϕ) plane (Fig. 1) gives the exact graph of the bifurcation diagram for fixed points (potential $V_d = d^{-2}$). Inspecting this bifurcation diagram, some anomalies are evident. Their study will be the topic of the next sections (Figs. 2–6).

IV. ANOMALOUS BIFURCATION PHENOMENA

As we now have a dynamical system and have determined all the fixed points, it is natural to study how these fixed points are generated or destroyed when varying the parameter G. Before applying standard methods we have to note

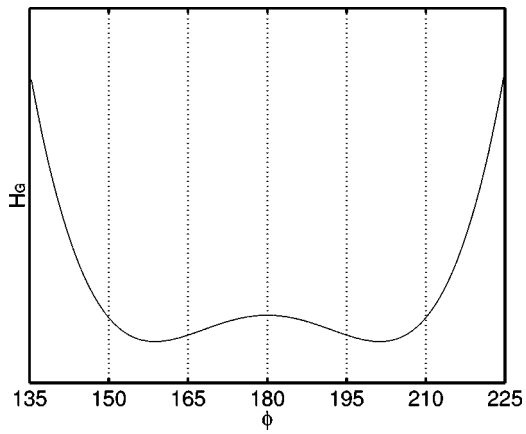

FIG. 4. Inhibitory potential for a spiral pattern with a divergence angle corresponding to 180° and for $G = 0.77$ (angles in degrees). The function has still an extremum at 180°, but now it is a maximum.

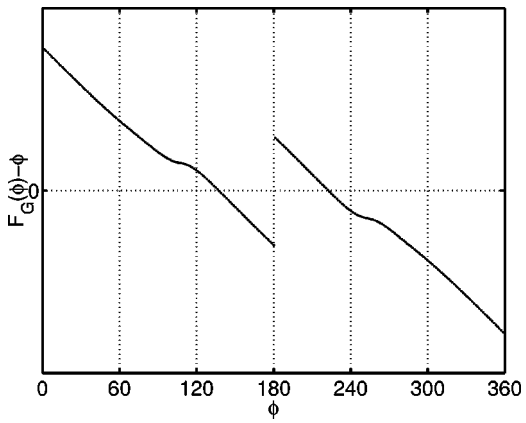

FIG. 5. Plot of the function $F_G(\phi)-\phi$ for $G=0.48$ (values of ϕ in degrees). As G is further reduced, two symmetric folds begin to form (around $\phi=110°$ and 250°).

that the model considered is not continuous. We will proceed in two steps.

(1) We will find the conditions under which the map is at least locally continuous. In these cases, we will expect usual phenomena.

(2) Besides usual bifurcations, we have to expect some nonstandard bifurcation phenomena related to the discontinuities. We will investigate these anomalies.

A. Origin of discontinuities

To study the discontinuities, we have to imbue our system with a topology. Thus we use the complex notation for points in phase space, and we introduce a usual norm for succession:

$$\|x\|=\sum_{k=0}^{\infty} a^{-k}|x_k|, \quad a>1. \tag{27}$$

Calling T the map, we will use as a necessary and sufficient condition for continuity in a point $\overline{x}$:

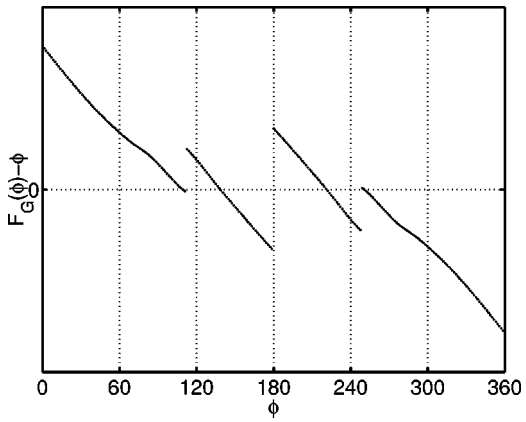

FIG. 6. Plot of the function $F_G(\phi)-\phi$ for $G=0.38$ (values of ϕ in degrees). Anomalous fold bifurcation: the two folds of Fig. 5 now touch the zero axis, giving rise to new fixed points. However, the fold has already broken into a discontinuity. Instead of the saddle-node pair we have a solution and a discontinuity.

$$\lim_{x\to\overline{x}}\|T(x)-T(\overline{x})\|=0. \tag{28}$$

Hence we have to evaluate Eq. (28). To do this, we start rewriting explicitly the map [note also that $x=(\theta,b)$ and $\overline{x}=(\overline{\theta},\overline{b})$]:

$$\begin{aligned} &x\to Tx,\\ &\theta_0\to 0,\\ &\theta_n\to\theta_{n-1}-f_G(\theta,b), \quad n>0,\\ &b_0\to 1,\\ &b_n\to b_{n-1}, \quad n>0. \end{aligned} \tag{29}$$

Then, for simplicity setting $\phi=f_G(\theta,b)$ and $\overline{\phi}=f_G(\overline{\theta},\overline{b})$, and evaluating the norm:

$$\begin{aligned} &\lim_{x\to\overline{x}}\|T(x)-T(\overline{x})\|\\ &\quad=\lim_{x\to\overline{x}}\sum_{k=1}^{\infty} a^{-k}|b_{k-1}e^{i(\theta_{k-1}-\phi)}-\overline{b}_{k-1}e^{i(\overline{\theta}_{k-1}-\overline{\phi})}|\\ &\quad=\lim_{x\to\overline{x}}\lim_{N\to\infty}\sum_{k=1}^{N} a^{-k}|b_{k-1}e^{i(\theta_{k-1}-\phi)}\\ &\qquad-\overline{b}_{k-1}e^{i(\overline{\theta}_{k-1}-\overline{\phi})}|. \end{aligned} \tag{30}$$

Now we observe that we can always choose a (sufficiently small) neighborhood of $\overline{x}$ in which for every x we have

$$b_k=\overline{b}_k, \quad \forall k\leqslant N$$

(otherwise $\|x-\overline{x}\|\leqslant a^{-N}$). Hence, close enough to this (e.g., in a radius of $\overline{x}$ less than a^{-N}) we have

$$\begin{aligned} &\sum_{k=1}^{N} a^{-k}|b_{k-1}e^{i(\theta_{k-1}-\phi)}-\overline{b}_{k-1}e^{i(\overline{\theta}_{k-1}-\overline{\phi})}|\\ &\quad=\sum_{k=1}^{N} a^{-k}|e^{i(\theta_{k-1}-\phi)}-e^{i(\overline{\theta}_{k-1}-\overline{\phi})}|. \end{aligned} \tag{31}$$

Exchanging the limits in Eq. (30) we can see that

$$\lim_{x\to\overline{x}}\|T(x)-T(\overline{x})\|=0\Leftrightarrow\lim_{x\to\overline{x}}|\phi-\overline{\phi}|=0. \tag{32}$$

The main consequence of (32) is that now we have isolated the discontinuities, and we need to study them on a real function instead of an infinite set of equations. Explicating ϕ, we have

$$\begin{aligned} \phi=f_G(\theta,b)&=\mathcal{M}_\alpha(H_{\theta,b,G}(\alpha))\\ &=\mathcal{M}_\alpha\left(\sum_{k=0}^{\infty} V_{kG}(\alpha-\theta_k)b_k\right). \end{aligned} \tag{33}$$

Checking the continuity of Eq. (33) as in the previous case shows that H depends continuously on x. This, however,

is not true for the $\mathcal{M}$ operator. In particular a necessary condition for a discontinuity will be that H has a minimum with zero second derivative or at least two equivalent minima. Here we do not need more than a necessary condition. To prove that the condition is also sufficient we would have to prove that varying the G parameter the inhibitory potential is perturbed generically. So we can conclude the following.

Proposition 3. Consider in the dynamical system of proposition 1, an equilibrium point with divergence angle ϕ. Then the system is locally continuous if the following conditions both hold:

(1) There is only one absolute minimum (i.e., there are not equivalent minima).

(2) The absolute minimum is not degenerate:

$$H''_{\theta,b,G}(\phi) \neq 0. \tag{34}$$

We make the following remarks.

(1) Proposition 3 will be used in two ways. First, it states a sufficient condition under which the system is continuous. This will be required essentially for the computation of the Jacobian. Second, it defines a region (the space where the condition does not hold) where we have to expect unusual bifurcation phenomena to appear.

(2) The condition is sufficient. To prove that the condition is also necessary we would have to show that varying the G parameter the inhibitory potential is perturbed generically. Although this seems reasonable (and is observed in numerical simulation), we limit our analysis to the sufficiency.

(3) If the above conditions hold, the system is at least continuous. However, as will be shown in Appendix B using the implicit function theorem, the system is also differentiable as many times as the first derivative of the inhibitory potential.

B. Anomalous bifurcations due to discontinuities

Now we investigate the effect of discontinuity on the appearance and disappearance of equilibria. Most of the analysis will be performed studying numerically the behavior of the real function (26) for different values of G (see Fig. 1). Looking at the bifurcation diagram of fixed points, there are at least two anomalous things that are evident. The first is the interruption of the π branch (at $G \sim 0.79$). The second one is the abrupt births of branches following the golden branch. We remark that in this diagram all fixed points, stable and unstable, are plotted. So the missing solutions do not collide with other solutions, nor do they stop because of a change in stability (for example by a Neimark-Saker or period-doubling bifurcation). They are simply removed. To understand this we study Eq. (26) and follow the π branch for decreasing G (Figs. 2–6). Calculating eigenvalues (see Appendix B), we find that the solution becomes unstable, giving rise to two nodes (Fig. 2). Then the tangency of Eq. (26) becomes infinite at the point of disappearance, and a discontinuity arises (Fig. 3). The reason for this is simple: in this point the inhibitory potential for a spiral with divergence angle of π changes the concavity, becoming a maximum (Fig. 4); however, this, as described in Sec. IV A, is a condition for a discontinuity. Calculations for obtaining analytically this point, for different potentials, can be found in Ref. [16].

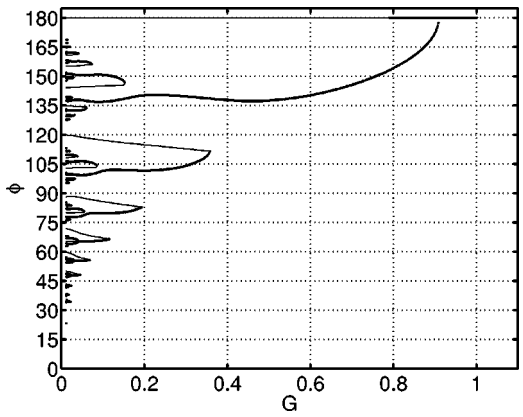

FIG. 7. Bifurcation diagram of fixed points and singularities (in degrees) vs G.

To understand the other bifurcations, we can again follow Eq. (26) after the first bifurcation for decreasing values of G. Then we find that a fold appears (Fig. 5) and touches the $F_G - \phi = 0$ axis at the bifurcation point. The only difference from a typical fold bifurcation is that before the contact a discontinuity develops (Fig. 6). The discontinuity is of the same type as for the π-branch case (zero second derivative). Thus we have a typical case, in which after a first symmetry-breaking bifurcation other bifurcations occur from the same phenomenon; however as now the system is no longer symmetric, the bifurcations become generic (the break of symmetry acts as a generic perturbation). Usually, we have pitchforks that are changed into folds. In our case we have the same situation, with the only difference being the presence of a discontinuity that removes the unstable solution.

Summing up, the phenomenon for the second bifurcations is foldlike, with a collision between a stable solution and a discontinuity. The situation is displayed in Fig. 7. Actually, we can think of the discontinuities as generalized saddle solutions. This role is also confirmed if we compare the positions of the discontinuities in respect to a (section of a) basin of attraction: then we find that they define the boundaries, as usually saddles in fold bifurcations do. See Fig. 8.

V. STATIC APPROACH

Till now we have followed a dynamical approach for studying the phyllotactic model. However, there is also a static viewpoint, in which one tries to obtain the phyllotactic patterns by defining a function that measures the efficiency by which elements are put together. This can mean, for instance, how much they are exposed to light (leaves), or how closely they are packed together (seeds). Here our aim is not an investigation of the connections between the static approach and the dynamical one (see, for example, Ref [7] or [15]). Instead, we are interested in finding the ''hidden'' unstable patterns. We especially want to find a way to circumvent the discontinuities of the map described in Sec. IV. Since the discontinuities arise from the dynamics, to avoid them we study the system statically, deriving a potential-like function for our system. The function we will look for shall

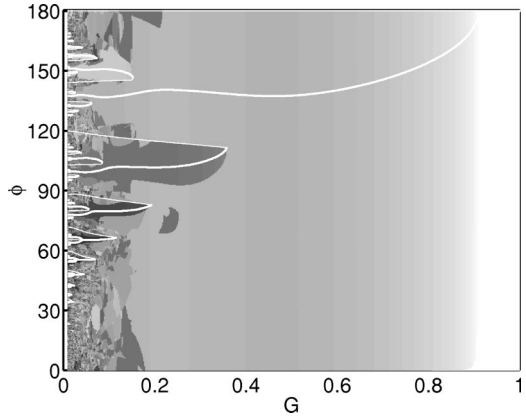

FIG. 8. Singularities (degrees) as boundaries of the basins of attraction. For each point, a spiral is first constructed with ϕ as a divergence angle, and G as a parameter. The color represents the divergence angle of the final pattern reached. Singularities seem to bound the basins, as saddle solutions in saddle-node bifurcations usually do.

have all fixed points in its extrema. The main advantage of this approach is that the class of extrema is larger than the one containing fixed points, and now there is no discontinuous dynamics that ''filters'' it. As we shall see, using all extrema we will be able to find the missing saddle points and to construct a typical, continuous bifurcation scenario.

A. Deduction

We want to find a function by which all fixed patterns are extrema. We proceed as follows.

The relation for fixed points is given by Eq. (26), that is,

$$F_G(\phi)=\phi,$$

where

$$F_G(\phi):=f_G(\theta,b),$$

$$\theta_n=-n\phi, b_n=1, \quad n\geqslant 0.$$

F_G is the function that gives the position of the absolute, leftmost minimum of the inhibitory potential generated by a spiral given the divergence angle. Writing F_G explicitly gives

$$F_G(\phi)=f_G(\{\theta_k=-k\phi\},\{b_k=1\})=\mathcal{M}_\alpha(H_{\theta,b,G}(\alpha))$$
$$=\mathcal{M}_\alpha\left(\sum_{k=0}^{\infty} V_{kG}(\alpha+k\phi)\right).$$

The positions of the minima are contained in the set of the zero first derivative points, and thus we differentiate with respect to α and equate the result to zero. Also, as we are looking for fixed points, we apply condition (23), that is, the position of the minimum and the divergence angle of the spiral must be the same:

$$\left(\frac{d}{d\alpha}\sum_{k=0}^{\infty} V_{kG}(\alpha+k\phi)\right)\Bigg|_{\phi=\alpha}=0. \tag{35}$$

The set of solutions of Eq. (35) contains all the fixed patterns. The next step is to rewrite Eq. (35) as the derivative of a function:

$$\frac{d}{d\alpha}S_G(\alpha)=\left(\frac{d}{d\alpha}\sum_{k=0}^{\infty} V_{kG}(\alpha+k\phi)\right)\Bigg|_{\phi=\alpha}. \tag{36}$$

It is not difficult to obtain an explicit form for S_G:

$$\left(\frac{d}{d\alpha}\sum_{k=0}^{\infty} V_{kG}(\alpha+k\phi)\right)\Bigg|_{\phi=\alpha}=\left(\sum_{k=0}^{\infty} V'_{kG}(\alpha+n\phi)\right)\Bigg|_{\phi=\alpha}$$
$$=\sum_{k=0}^{\infty} V'_{kG}((k+1)\alpha); \tag{37}$$

thus

$$S_G(\phi)=\int_0^{\phi}\sum_{k=0}^{\infty} V'_{kG}((k+1)\alpha)d\alpha$$
$$=\sum_{k=0}^{\infty}\frac{1}{(k+1)}V_{kG}((k+1)\phi). \tag{38}$$

We can now conclude the following

Proposition 4. The dynamical system of Proposition 1 admits a smooth function $S_G(\phi)$ for which all fixed points are extrema. $S_G(\phi)$ has the form

$$S_G(\phi):=\sum_{k=0}^{\infty}\frac{1}{(k+1)}V_{kG}((k+1)\phi). \tag{39}$$

We make the following remarks.

(1) Equation (39) resembles a potential, as all fixed points of the dynamical system correspond to extrema. It can be seen as a measure of the packing efficiency minimized by the system.

(2) To obtain Eq. (39) we have used a necessary but not sufficient condition: in fact by doing this we consider not only the absolute, leftmost minimum, but also relative minima, maxima, and inflection points with vanishing slope. In this way, we have avoided the discontinuities of the $\mathcal{M}$ operator, and (as shown in the Sec. V B), we are now able to find the patterns deleted by the discontinuities.

B. Maxima of the packing energy as saddle solutions

Now we came back to the problem of the missing saddle solutions. We have noted that the fixed points of the dynamical system defined in proposition 1 do not coincide but are contained in the set of the extrema of the S_G function. In Fig. 9 we plot minima and maxima of S_G. We can observe that there are no more discontinuities. In fact, in the static approach we do not have to calculate the absolute minimum, and thus all operators are continuous. Now let us come back to the problem of the ''missing'' unstable solutions. If we compare Fig. 1 with Fig. 9 we can see that, in addition to the stable solutions, new solutions appear, corresponding to maxima or inflection points with vanishing slope of S_G. They collide with the stable solutions as in a typical fold bifurcation. Considering the derivation of S_G, a solution be-

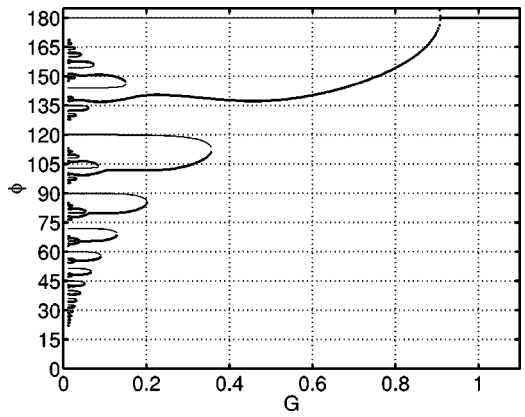

FIG. 9. Maxima and minima of the function S_G (degrees). Minima are plotted more darkly. The extrema of S_G include all equilibria of the system. The complementary points correspond to patterns in which the inhibitory potential has a maximum, and are thus absent from Fig. 1 (the $\mathcal{M}$ operator only gives minima).

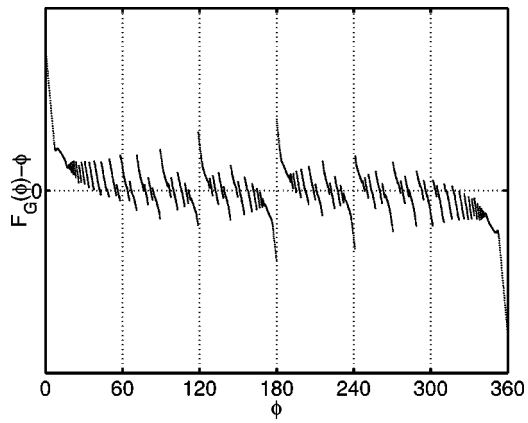

FIG. 10. Plot of the function $F_G(\phi)-\phi$ for $G=0.05$ (value of ϕ in degrees). Where $G\to 0$, the behavior of the function becomes complex, and a discontinuity seems to appear for every rational value of $\phi/360°$, and a zero for every noble number.

longs to Fig. 9 and not to Fig. 1 if it corresponds to a spiral pattern in which the inhibitory potential has a maximum or an inflection point, and not a minimum, when evaluated as a function of the divergence angle.

VI. CONCLUSIONS

In Sec. II the phyllotactic algorithm was translated into a well defined dynamical system, and the result is summarized in proposition 1 where a discrete-time, infinite-dimensional dynamical system is obtained. Then Sec. III imposed the condition for a point to be fixed and deduced two equations that characterized both stable and unstable patterns (proposition 2). In particular, from these equations it was seen that growth and inhibitory interactions play two independent roles: the growth mechanism (that is, the fact that one primordium is added and the other ones are pushed away) bounds the choice of fixed patterns to the class of spirals; meanwhile, the inhibitory interaction determines the divergence angle and (especially) the bifurcations of the solutions through a one-dimensional function [Eq. (23)]. Figure 1 summarizes these results, showing the full bifurcation diagram for fixed points as the loci of zeroes for Eq. (23).

Then bifurcations were studied. First, Sec. IV A showed that the map is not continuous. Thus we started to look for conditions under which the system is at least locally continuous, and where usual phenomena arise. Sufficient conditions for local continuity were obtained in proposition 3, showing that discontinuities in the dynamical system are entirely determined by Eq. (23). Then, in Sec. IV, anomalous bifurcations due to discontinuities were studied. A foldlike phenomenon was found where, instead of the usual saddle-node pair, a stable solution collides with a discontinuity. Numerical calculations displayed in Fig. 8 showed that the discontinuities also play the role of saddle solutions as boundaries of the basins of attraction.

Aiming to recover the usual scenario, Sec. V approached the model in a static way, trying to circumvent the singularities due to the dynamics. To do so, it (constructively) showed the existence of a potential-like function, for which all fixed points are extrema. However, the class of extrema is larger than fixed points admitted by the dynamical system. Considering all of these a new family of patterns appears, that is connected to fixed points like in a usual fold scenario. The results are summarized in proposition 4 and in Figs. 9 and 10.

Finally, Appendixes A and B give a method by which the dynamical system can be approximated (in C^0 topology) by a finite-dimensional one. For this latter system, an explicit form for the Jacobian is given, allowing one to calculate eigenvalues.

The main aim of this work has been to show that the phyllotactic algorithm can be translated into a dynamical system and then benefits from the already developed, analytical tools from dynamical systems theory. From this point of view, Secs. III–V are just some possible examples. Other further possibilities can be the study of Eq. (23) with center manifold theory, to understand the reduction from an infinite-dimensional space to a one-dimensional equation; an extension of the analysis of Sec. III to cycles; a theoretical analysis of the anomalous bifurcation, that here is mainly numerical; an investigation of the discontinuities of the system, aimed at understanding if they have a biological meaning or are just an artifact of a simplified model; and many others. We consider two possible further approaches to be of particular importance.

The use of center manifold theory should give a good insight into the mechanisms by which a global property (a common divergence angle) is selected by the local interactions among leaves and the apex.

We have shown that locally, in C^0 topology, the system can always be approximated by a system with a finite number of leaves. This has been useful to compute the Jacobian and then to estimate the eigenvalues. However, there is a deeper meaning. As the system is qualitatively equivalent to a model with a finite number of elements, it follows that each bifurcation is characterized by a critical dimension number (the minimum number of leaves) below which it cannot be observed.

ACKNOWLEDGMENTS

F.d'O. gratefully acknowledges the hospitality of the Chaos Group at the Technical University of Denmark, and

the Chemistry Department, University of Copenhagen, that partly supported the work.

APPENDIX A: A FINITE APPROXIMATION

The dynamical system obtained in Sec. II is useful in obtaining an exact relation for fixed points. However, it is infinite dimensional. This can be a problem, for instance, when calculating eigenvalues, as their number is also in principle infinite. In practice, noting that the inhibitory contribution of each leaf decreases with the age, a natural idea is to truncate the infinite-dimensional system considering only leaves younger than a certain age N (that we can expect will depend on G). This approach can be formalized, showing that a truncated system is a ''good'' approximation in the sense that it is close to the original one in C^0 as much as we want, providing that N is sufficiently large. An important consequence of this is that, invoking genericity, the two system will share the same (at least local) bifurcation scenario. Moreover, this approach will give us a way to estimate the eigenvalues, even if apparently the two systems have a different dimension, and thus a different number of eigenvalues.

We will proceed as follows. First we will write the truncated system in a form by which it can be compared to the original one. Then we will measure the distance between the two. Finally, we explicitly derive a formula for the Jacobian of the truncated system. In all of this section, we require the systems to be at least continuous. This means that our results will apply under the (sufficient) continuity conditions of proposition 3, and that the results will have a *local* validity only.

Using the same notation as in proposition 1 for the truncated system, we can formally write the phase space as

$$x_N \in X_N \Leftrightarrow x_N = \{\theta_N, b_N\}, \tag{A1}$$

$$\theta = \{\theta_k\}_{k=0}^{N}, \quad b = \{b_k\}_{k=0}^{N}, \quad \theta_k \in [0, 2\pi), \quad b_k \in \{0,1\} \tag{A2}$$

Then the equation for the map becomes:

$$x_N \rightarrow T_N x_N, \tag{A3}$$

$$\begin{aligned} &\theta_0 \rightarrow 0, \\ &\theta_n \rightarrow \theta_{n-1} - f_{G,N}(\theta, b), \quad 0 < n < N, \end{aligned} \tag{A4}$$

$$\begin{aligned} &b_0 \rightarrow 1, \\ &b_n \rightarrow b_{n-1}, \quad 0 < n < N. \end{aligned} \tag{A5}$$

where $f_{G,N}$ is obtained by truncating the series of Eq. (14) to the N-th term.

However, we cannot compare two systems acting on different dimensional spaces. Thus we need to add ''dummy'' (i.e., decoupled) equations for the other variables. To do so we suspend Eq. (A1) in the infinite-dimensional space X in the following way:

$$x \rightarrow T_N x, \tag{A6}$$

$$\begin{aligned} &\theta_0 \rightarrow 0, \\ &\theta_n \rightarrow \theta_{n-1} - f_G(\theta, b), \quad 0 < n < N, \\ &\theta_n \rightarrow 0 \quad n \geqslant N, \end{aligned} \tag{A7}$$

$$\begin{aligned} &b_0 \rightarrow 1, \\ &b_n \rightarrow b_{n-1}, \quad 0 < n < N, \\ &b_n \rightarrow 0, \quad n \geqslant N, \end{aligned} \tag{A8}$$

Now we will compare the truncated system as defined in Eq. (A6) with the original one (proposition 1). In particular, we want to show that in the C^0 topology of continuous maps (locally) defined on X the two systems are ε close; that is, that for sufficiently large N,

$$\| T_N - T \| < \varepsilon, \tag{A9}$$

or, in other words,

$$\lim_{N \rightarrow \infty} \| T_N - T \| = 0. \tag{A10}$$

Of course we have to specify the norm

$$\| T_N - T \| = \sup(\| T_N x - T x \|)_{x \in \Omega}, \tag{A11}$$

where Ω is the (open) set where the local conditions of proposition 3 hold:

$$\begin{aligned} &\lim_{N \rightarrow \infty} \sup(\| T_N x - T x \|)_{x \in \Omega} \\ &= \lim_{N \rightarrow \infty} \left(\sup \left(\sum_{k=1}^{N} a^{-k} | b_{k-1} e^{i(\theta_{k-1} - \phi)} \right.\right. \\ &\quad \left.\left. - b_{k-1} e^{i(\theta_{k-1} - \phi_N)} | \right) + \sum_{k=N+1}^{\infty} a^{-k} \right) \\ &= \lim_{N \rightarrow \infty} \left(\sup \left(\sum_{k=1}^{N} a^{-k} b_{k-1} | e^{i(-\phi)} - e^{i(-\phi_N)} | \right) \right. \\ &\quad \left. + \sum_{k=N+1}^{\infty} a^{-k} \right). \end{aligned} \tag{A12}$$

We can drop the second term of Eq. (A12), as it is the remainder of a geometric convergent series. Also, we can overestimate [Eq. (A12)], considering all b_k different from zero:

$$\begin{aligned} &\lim_{N \rightarrow \infty} \sup(\| T_N x - T x \|)_{x \in \Omega} \\ &\leqslant \lim_{N \rightarrow \infty} \sup \left(\sum_{k=1}^{N} a^{-k} | e^{i(-\phi)} - e^{i(-\phi_N)} | \right) \\ &\leqslant \left(\frac{1}{1 - 1/a} \right) \lim_{N \rightarrow \infty} \sup(| e^{i(-\phi)} - e^{i(-\phi_N)} |). \end{aligned} \tag{A13}$$

But Eq. (A13) converges to zero, as, under continuity conditions of proposition 3, $\phi_N \to \phi$ as $N \to \infty$. Thus we can conclude the follows

Proposition 5. Consider the dynamical system (17) (full system), the parametric dynamical system (A6) (truncated system) and the norm of Eq. (A11). Then, under the continuity conditions of proposition 3, the two systems are locally $\varepsilon - C^0$ close; that is, for every $\varepsilon > 0$ there exists an $N_0 > 0$ such that

$$\|T_N - T\| < \varepsilon, \quad \forall N > N_0. \tag{A14}$$

We make the following remarks.

(1) The result is local (in a region in phase and parameter space where the system is continuous).

(2) Proposition 5 has an obvious practical meaning. Invoking it and genericity, we can study the behavior of the phyllotactic system considering only a finite-dimensional model. In this work we will not go further. However, there is another interesting result that emerges from it. The truncated system is a system in which only the contribution of the last N leaves is retained. This means that there are (integer) critical values of N (that is, a critical number of leaves) that characterize local bifurcations, a sort of intrinsic dimension of the phenomena. Thus a bifurcation also corresponds to a critical value of G by which this number jumps from an integer to another. Inspecting Eq. (39) and Fig. 9, it is not difficult to hypothesize that this number must increase with decreasing G, and must be greater than the number of equilibria. In fact, the S_G function must have a minimum for each equilibrium, and it is the sum of single maximum functions. Preliminar, numerical calculations confirm this hypothesis.

(3) Proposition 5 guarantees that it is *always* possible to approximate the system with a finite one. However, it does not give a method to estimate how large N must be in order to maintain the same bifurcation structure.

APPENDIX B: JACOBIAN

Here we derive a formula to compute explicitly the Jacobian for the approximated system. Applying the result from Appendix A, we can then use it to approximate eigenvalues of the original system.

We start by rewriting the equations that define the truncated system, adopting for simplicity the notation $\phi = f_G(\theta, b)$:

$$x \to T_N x, \tag{B1}$$

$$\begin{aligned} &\theta_0 \to 0, \\ &\theta_n \to \theta_{n-1} - \phi, \quad 0 < n < N, \\ &\theta_n \to 0 \quad n \geqslant N, \\ &b_0 \to 1, \\ &b_n \to b_{n-1}, \quad 0 < n < N, \\ &b_n \to 0, \quad n \geqslant N. \end{aligned} \tag{B2}$$

Now we shall proceed backwards in respect to the definition of the truncated system, observing that the dynamics of the first N coordinates is decoupled from the others. So we can decompose the map of Eq. (B1) into two operators, one acting on the first N coordinates, the other on the rest. It is easy to see that the second one is just a constant, thus having a null linear part (and thus all zero eigenvalues). Meanwhile, for the Jacobian part of the first operator we can write

$$J_{i,j} := \frac{\partial T_N^i}{\partial x_j}, \quad 0 \leqslant i, j \leqslant N. \tag{B3}$$

Using for x a complex notation as in Eq. (13), Eq. (B3) is well defined. However, we can simplify it if we consider that, after (at most) N steps, all the first N b_k are equal to 1. Thus if we will use the Jacobian on singularities (fixed points or cycles), we can restrict our calculation only to the angular coordinate, and thus write

$$J_{i,j} := \frac{\partial T_N^i}{\partial \theta_j}, \tag{B4}$$

Explicating T_N^i,

$$J_{0,j} = 0 \tag{B5}$$

and

$$J_{i,j} = \frac{\partial}{\theta_j}(\theta_{i-1} - \phi) = \delta_{i-1,j} - \frac{\partial \phi}{\partial \theta_j}, \quad 0 < i \leqslant N. \tag{B6}$$

Here $\delta_{i-1,j}$ denotes Kronecker's delta.

Hence we have to compute

$$\frac{\partial \phi}{\partial \theta_j}. \tag{B7}$$

Explicating ϕ, we have

$$\phi = f_G(\theta, b) = \mathcal{M}_\alpha(H_{\theta,b,G}(\alpha)). \tag{B8}$$

Thus, the following must also hold:

$$\frac{d}{d\alpha} H_{\theta,b,G}(\alpha)\big|_{\alpha=\phi} = 0. \tag{B9}$$

That is, ϕ is a solution of $H'_{\theta,b,G}(\alpha) = 0$. Now, under conditions of proposition 3 we can apply the implicit function theorem and, choosing $\alpha, \theta_0, \ldots, \theta_N$ as independent variables, claim that

$$H'_{\theta,b,G}(\alpha) = 0$$

implies the (local) existence of an implicit function

$$\alpha = \alpha(\theta_0, \ldots, \theta_N), \tag{B10}$$

differentiable as many times as H', for which

$$\frac{\partial \alpha}{\partial \theta_j} = -\frac{\partial H'_{\theta,b,G}}{\partial \theta_j}\left(\frac{\partial H'_{\theta,b,G}}{\partial \alpha}\right)^{-1}. \tag{B11}$$

So we can insert Eq. (B11) into Eq. (B6), and obtain

$$J_{0,j} = 0, \tag{B12}$$

$$J_{i,j}=\delta_{i-1,j}+\frac{\partial H'_{\theta,b,G}}{\partial\theta_j}\left(\frac{\partial H'_{\theta,b,G}}{\partial\alpha}\right)^{-1},\quad 0<i\leqslant N. \tag{B13}$$

Explicating H',

$$H'_{\theta,b,G}(\alpha)=\frac{d}{d\alpha}\left(\sum_{k=0}^{N}V'_{kG}(\alpha-\theta_k)\right), \tag{B14}$$

and defining two coefficients

$$C_j:=\frac{\partial H'_{\theta,b,G}}{\partial\theta_j}=-V''_{jG}(\alpha-\theta_j), \tag{B15}$$

$$A:=\frac{\partial H'_{\theta,b,G}}{\partial\alpha}=\sum_{k=0}^{N}(V''_{kG}(\alpha-\theta_k))=-\sum_{k=0}^{N}C_k, \tag{B16}$$

we thus obtain the following important relation that gives the Jacobian:

$$J_{0,j}=0, \tag{B17}$$

$$J_{i,j}=\delta_{i-1,j}-\frac{C_j}{\sum_{k=0}^{N}C_k},\quad 0<i\leqslant N. \tag{B18}$$

We make the following remarks.

(1) Although for the Jacobian we are interested in the first derivatives only, the implicit function theorem allows us to obtain further derivatives, as far as the inhibitory potential is differentiable.

(2) Inspecting Eq. (B17) shows that the Jacobian is a matrix with ones on the diagonal below the principal one, plus coefficients $(-C_j/A)$ that are the same for all rows (they do not depend on i). Although this expression is enough for explicitly obtaining the Jacobian, the simple and compact form of Eq. (B17) suggests the possibility of obtaining conditions on the eigenvalues. However, we will not pursue this investigation in the present paper.

(3) The use of the implicit function theorem to obtain the partial derivative of T_N can also be made, in the same way, for the full system, replacing sums with series and checking convergences (that, for instance, is always obtained for the class of potentials of Sec. II A).

[1] L. Bravais and A. Bravais, Ann. Sci. Nat. Second Series, **7**, 42 (1837).
[2] I. Adler, D. Barabe, and R.V. Jean, Ann. Bot. (London) **80**, 231 (1997).
[3] F.J. Richards, Philos. Trans. R. Soc. London, Ser. B **235**, 509 (1951).
[4] W. Hofmeister, *Allgemeine Morphologie der Gewasche* (Engelman, Leipzig, 1868).
[5] G.P. Bernasconi and J. Boissonade, Phys. Lett. A **232**, 224 (1997).
[6] P.B. Green, C.S. Steele, and S.C. Rennich, Ann. Bot. (London) **77**, 515 (1996).
[7] C. Marzec and J. Kapraff, J. Theor. Biol. **103**, 201 (1983).
[8] S. Douady and Y. Couder, Phys. Rev. Lett. **68**, 2098 (1992).
[9] S. Douady and Y. Couder, J. Theor. Biol. **178**, 255 (1996).
[10] S. Douady and Y. Couder, J. Theor. Biol. **178**, 275 (1996).
[11] S. Douady and Y. Couder, J. Theor. Biol. **178**, 295 (1996).
[12] A.J. Koch, J. Guerreiro, G.P. Bernasconi and J. Sadik, J. Phys. I **4**, 187 (1994).
[13] L.S. Levitov, Europhys. Lett. **14**, 533 (1991).
[14] L.S. Levitov, Phys. Rev. Lett. **66**, 224 (1991).
[15] M. Kunz, Commun. Math. Phys. **169**, 261 (1991).
[16] F. d'Ovidio, C.A. Andersen, C.N. Ernstsen, and E. Mosekilde, Math. Comp. Sim. **49**, 41 (1999). .